Timing Synchronization of the WIND-FLEX OFDM Prototype

Mika Lasanen, Jukka Rautio, Mauri Nissilä

VTT Electronics, Telecommunication Systems,
P.O. Box 1100 (Kaitoväylä 1), FIN-90571 Oulu, Finland
Tel: +358 8 551 2291, email: Mika.Lasanen@vtt.fi

ABSTRACT

Timing synchronization of an early WIND-FLEX prototype is discussed in this paper. Simulation results for different low-complexity timing synchronization metrics are given in an AWGN (additive white Gaussian noise) channel. Simulations take into account frame detection via a threshold comparison followed by symbol timing estimation using a maximum search. Training symbols are fixed. A novel low-complexity metric reaches equal or better results than the maximum correlation (MC) metric, if we require optimal timing. Furthermore, nearly identical performance as with the maximum normalized correlation (MNC) metric is achieved, if threshold 0.4 or 0.6 is used.

I. INTRODUCTION

In the WIND-FLEX project, research and development work on adaptive, flexible and re-configurable high bit rate indoor WLAN modems at 17 GHz is carried out. The emphasis is on OFDM systems that fit well to high bit rate WLAN systems as HIPERLAN/2 and IEEE802.11a standards show [1].

In the project, we build first a transmitter receiver pair, an early prototype, to test a basic OFDM implementation mainly in an AWGN channel. Then, more sophisticated features are included in the implementation to achieve the final demonstrator.

A timing synchronizer of OFDM systems must usually estimate both the start of an individual symbol and packet of symbols, i.e., a frame. Sensitivity of OFDM systems to timing inaccuracies is discussed in [1]. Smaller timing errors make it possible to use a shorter guard interval (GI), i.e., a cyclic prefix. From the literature we can see that most often used methods exploit repeated sample sequences or symbols [1,2]. OFDM systems offer repeated sample sequences in a systematic way by the GI. To attain a faster acquisition repeated training symbols are often used [1,2,3]. Another method utilizes a well-known matched filter principle [1]. A comparison between these two principles in an OFDM system is presented in [4].

In this paper, we show floating-point timing synchronization simulation results for the WIND-FLEX prototype over an AWGN channel. We compare few timing metrics simulated in [5] with a novel metric in our system model. Our study is limited to metrics that offer a low complexity. In our case we divide timing synchronization into two phases, namely frame detection and symbol timing. In frame detection, a metric and a threshold are used to find roughly the frame start, i.e., the first training symbol. Then, symbol timing of the same symbol is achieved by a maximum search over a window period. Similar approach can be found in [4]. In simulations we take into account the whole frame structure of the WIND-FLEX prototype and the control architecture of the timing synchronizer.

The structure of this paper is as follows. Signal model including generation of OFDM symbols and the frame structure is shown in Section II. Then, we present used timing synchronization procedures in Section III. These cover the control architecture of the timing synchronizer, relevant timing metrics from the literature and definition of metrics used in simulations. Simulation results are shown in Section IV, where we compare metrics with few example threshold values at different SNRs (signal-to-noise ratio). Finally, in Section V some conclusions are given.

II. SIGNAL MODEL

A. Generation of OFDM Symbols

An OFDM symbol consists of N orthogonal subcarriers. Subcarrier spacing Df equals to $1/T_S$, where T_S is symbol period. Some subcarriers are zero-valued to ease filtering. Others carry data encoded in subsymbols X_k. The baseband OFDM symbol may be generated as

$$x(n) = \sum_{k=-L}^{L-1} X_k \exp\left(j2p \frac{nk}{N} \right), \qquad (1)$$

where n=0, 1 ..., N-1 is a sample index and L=N/2. Sample interval is defined as T_S/N. Eq. (1) is often implemented by an IFFT. To guarantee that received subcarriers are orthogonal after a multipath channel each OFDM symbol begins with a GI of N_g samples. These samples are copies of $x(N\text{-}N_g)$, ..., $x(N\text{-}1)$. Ideally, the GI should be longer than a channel impulse response. The GI may also be used to compensate timing inaccuracies.

B. Frame Structure

Frame structure of the WIND-FLEX prototype is shown in Fig. 1. In the beginning of the frame, we have three training symbols. The first training symbol consists of two short synchronization patterns (SP1). This is used

both in timing and coarse CFO (carrier frequency offset) synchronization, i.e., when the CFO can be multiple subcarrier spacings. Two remaining synchronization patterns (SP2) are utilized to estimate the fine CFO and the channel. Note that the first training symbol does not include GI. Instead, zero sample values are inserted. 175 data symbols follow training symbols. Frames are transmitted sequentially.

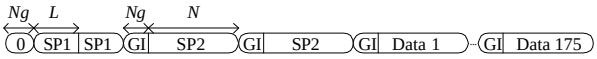

Fig. 1. Frame structure.

III. TIMING SYNCHRONIZATION PROCEDURES

The control architecture of the discussed timing synchronizer is presented in Fig. 2. Blocks 2 and 3, i.e., frame detection and symbol timing, are not active at the same time. Activation of these blocks is shown by dashed lines. Solid lines connect signals from one block to another.

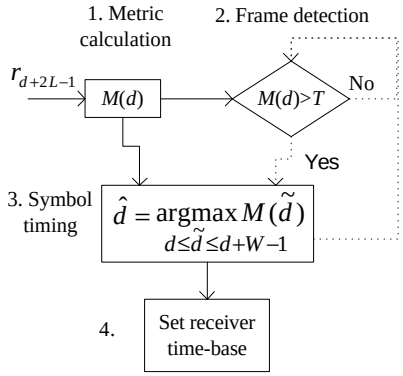

Fig. 2. Flowchart for timing synchronization.

A timing metric $M(d)$ defined in the following subsections is calculated in block 1 for each received complex baseband signal sample $r_i=s_i+n_i$ indexed with i and consisting of a signal s_i and a noise n_i component. Metric $M(d)$ uses $2L$ most recent samples. In block 2, each $M(d)$ is compared with a threshold T until a frame start is detected, i.e., $M(d)>T$. The detection activates block 3 and W timing metrics are compared. Estimated symbol timing is the time index of the maximum value of these $M(d)$, …, $M(d+W-1)$. A receiver can use this symbol timing and frame start estimate to locate all other symbols in the frame and set a receiver time-base (block 4).

After comparison of W timing metrics in block 3, block 2 is activated. This means that each frame is detected from scratch. Also a demodulation process of a correctly synchronized frame can be interrupted by a false alarm. One more drawback of the procedure is its high power consumption. On the other hand, a false alarm before a frame does not mean alone that this frame will be lost. This kind of synchronization control may be a flexible solution. It should work in different system models. For instance, a non-constant frame period a priori unknown to the receiver would be possible.

A. Timing Metrics from the Literature

In [3], a timing synchronization method suitable for the first training symbol of Fig. 1 was presented. The metric

$$M(d) = \frac{|P(d)|^2}{(R(d))^2} \tag{2}$$

uses the correlation of two subsymbols SP1

$$P(d) = \sum_{m=0}^{L-1} (r_{d+m}^* r_{d+m+L}) \tag{3}$$

and the energy of the second subsymbol SP1

$$R(d) = \sum_{m=0}^{L-1} |r_{d+m+L}|^2. \tag{4}$$

In [5] it has been demonstrated that the performance of (2) is improved by a slight modification

$$R_b(d) = \sum_{m=0}^{2L-1} |r_{d+m}|^2 \tag{5}$$

and having

$$M_b(d) = \frac{4|P(d)|^2}{(R_b(d))^2}. \tag{6}$$

We see that energy $R_b(d)$ considers all samples used in correlation (3). This maximum normalized correlation metric (MNC) is also used in [6].

Use of $|P(d)|$ or its squared value alone in timing synchronization was proposed in [7]. This is called as maximum correlation (MC) metric [5].

It is important to note that Eqs. (3)-(5) can be implemented by recursive formulas [3]. In addition, metrics (2) and (6) suit well in the threshold comparison because they have mainly values between 0 and 1.

We may calculate average value of $M(d)$ at the optimal timing instant d_{opt} as [3]

$$E[M(d_{\text{opt}})] = \frac{s_s^4}{\left(s_s^2 + s_n^2\right)^2}, \tag{7}$$

where squared signal variance is divided by the squared sum of signal and noise variances. Eq. (7) assumes that $M(d_{\text{opt}})$ can be approximated as a Gaussian random variable at high SNRs.

To have an example of how metric (6) behaves around the optimal timing instant we have plotted Fig. 3. We can see that the peak value does not differ very much from adjacent values. Thus, the threshold comparison can not estimate symbol timing alone. In the figure SNR is 6 dB. SNR is defined as

$$\text{SNR} = \frac{s_s^2}{s_n^2}. \tag{8}$$

B. Timing Metrics Used in Simulations

We define metrics M_1 to be used in simulations as

$$M_1(d)=M(d) \text{ or } M_{1,b}(d)=M_b(d), \quad (9)$$

where $M(d)$ and $M_b(d)$ are given in (2) and (6), respectively. Metrics M_2 are defined as

$$M_2(d) = |P(d)|^2 \text{ or } M_{2,b}(d) = 4|P(d)|^2 \quad (10)$$

and novel metrics M_3 as

$$M_3(d) = |P(d)|^2 - T(R(d))^2$$
$$\text{or} \quad (11)$$
$$M_{3,b}(d) = 4|P(d)|^2 - T(R_b(d))^2.$$

Eqs. (10) and (11) have two options. The first one is obtained from (2) and the second one from (6) by holding the frame detection criterion equalent for each metric. Thus, frame detection critera for all metrics are

$$M_1(d) > T \text{ or } M_{1,b}(d) > T$$
$$M_2(d) > T(R(d))^2 \text{ or } M_{2,b}(d) > T(R_b(d))^2 \quad (12)$$
$$M_3(d) > 0 \text{ or } M_{3,b}(d) > 0$$

Note that right-hand sides of presented inequalities act as the threshold in Fig. 2. The latter metrics may be called as *b* metrics ($M_{1,b}(d)$, $M_{2,b}(d)$, $M_{3,b}(d)$).

We can see that the use of metrics M_1 forces us to perform a division operation at a sampling rate. Metrics M_2 and M_3 offer a less complex implementation and metrics M_2 are the least complex ones.

We are interested in comparing performances of presented metrics in symbol synchronization accuracy. This maximum search has been simulated for MC metric (10), metric (2) and MNC metric (6) in [5].

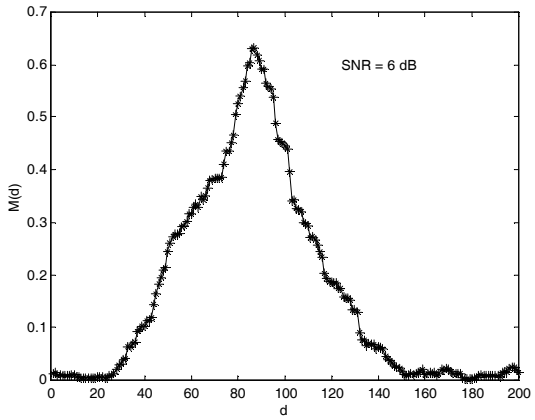

Fig. 3. Timing metric (6).

IV. SIMULATIONS

A. Simulation Parameters

In the WIND-FLEX project N=128 subcarriers are used in 50 MHz bandwidth. The latter value defines also sampling rate at baseband. GI consists of N_g=22 samples.

Subcarriers having indices k = –64, –63,...,–49, 0, 49, 50, …, 63 in (1) are assigned zero values in simulations. This leaves 96 subcarriers for data. Two short subsymbols SP1 are generated as in [3], i.e., every second subcarrier is zero-valued. For instance, two subcarriers around subcarrier k=0 are zero-valued. Training symbols are fixed and they have been designed to have low crest factors. Training symbols SP2 are BPSK encoded. Other symbols use QPSK. All data is random.

We have used a large value W=80 as a maximum search window. This is not optimized in simulations. One should note that if we have the high SNR, small T and W we will have many frame detections around the optimal frame timing (see Fig. 3). Also, we do not optimize threshold values because they are strongly dependent on the SNR. Instead, we use threshold values T=0.2, 0.4 and 0.6.

In simulations, we have assumed that a false alarm in frame detection taking place during W last samples of the frame does not cause a frame error to the current frame. An AWGN channel is used. We consider SNR values 0, 3, 6, 9, and 12 dB. Only four of these will be shown in each table. In the prototype we may use SNRs larger than about 6 dB, because we do not introduce channel coding. We do not consider CFO different from zero in simulations. Its effects on metric values may not be significant. CFO rotates $P(d)$ but does not change its amplitude. Also signal energy $R(d)$ is not affected by CFO.

For each simulation result, 100 000 frames has been generated. We obtained a correct timing estimate if it satisfied $|dt|<I$, where I can have integer values from 1 to 16. Case $|dt|<1$ means that the optimum timing instant d_{opt} has been estimated.

B. Simulation Results

In Table 1, we present values for (7) and simulated average values for metrics (2) and (6) at the optimal timing instant. We note that all values corresponding to the same SNR are nearly identical and values grow rapidly as SNR increases. As an example, we present histograms for simulated $M(d_{\text{opt}})$ values of metrics (2) and (6) at SNR of 3 dB in Figs. 4 and 5. Standard deviations of measurements are 0.081 for (2) and 0.054 for (6). One can see from figures that metric (2) gets more smaller values than (6). Thus, by using the MNC metric (6) instead of metric (2) we may detect more frames correctly by the threshold comparison and estimate symbol timing more accurately. Metric (6) is also closer to a Gaussian distribution at the SNR of 3 dB.

Table 1. Theoretical and simulated average values for metrics $M(d_{\text{opt}})$ and $M_b(d_{\text{opt}})$

	SNR (dB)				
	0	3	6	9	12
Eq. (7)	0.25	0.44	0.64	0.79	0.88
Eq. (2)	0.26	0.45	0.65	0.79	0.89
Eq. (6)	0.26	0.45	0.64	0.79	0.89

Table 2 includes simulation results for the case where T=0.2 and $R(d)$ is energy of 64 samples as in (4). The first percentage value tells the simulated probability that a frame is timing synchronized at the desired

accuracy and no false alarms occur during the frame. The second value shows all those cases where symbol synchronization has taken place in a desired window (false alarms possible). In this way we can see the effect of false alarms to the timing synchronization. Note that we present results for SNRs from 0 to 9 dB. The results show that there are no dramatic differences between various metrics when $|dt|<16$. However, M_2 produces better estimates when $|dt|<2$ or 3 and SNR is small. As SNR increases novel M_3 outperforms other metrics and especially M_2 if we require that $|dt|$ is small. We see also that the performance of metrics gets worse when SNR increases from 6 to 9 dB and we allow $|dt|<3$ or 16. A partial reason for this may be the fact that the used maximum search window W is too short for T=0.2 at high SNRs (compare to Fig. 3).

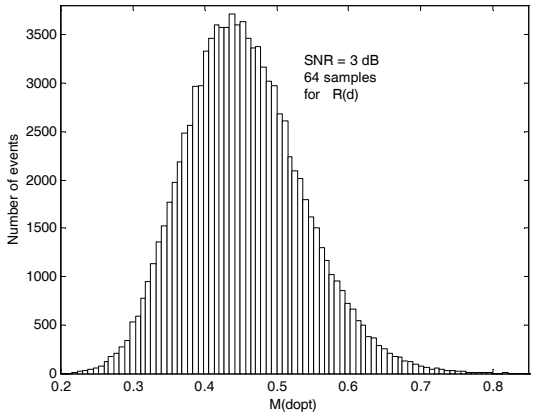

Fig. 4. Histogram for metric (2) at d_{opt}; SNR = 3 dB.

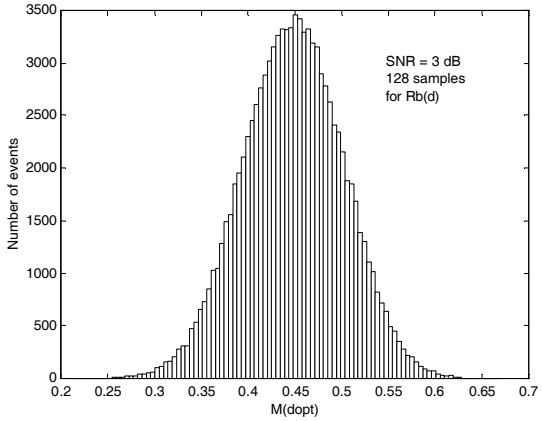

Fig. 5. Histogram for metric (6) at d_{opt}; SNR = 3 dB.

Table 3 shows corresponding results for which energy $R_b(d)$ considers 128 samples as in b versions of the metrics. One can see that the overall performance is improved compared to Table 2. There are only few exceptions with M_1 and M_3 if we demand that $|dt|<1$. Thus, we have used b versions of metrics for all following simulation results. Furthermore, we can see that about 95% of all frames are timing synchronized correctly with all methods if we accept $|dt|<3$ and have the SNR equal to or larger than 3 dB. At higher SNRs there are larger differences if we require $|dt|<1$. M_1 is the most accurate while M_2 gives the most modest results. When larger estimation error is allowed differences are modest. M_2 should be favored for cases where SNR is low (in our case SNR=0 dB); see also [5].

Table 2. Probabilities (%) of correct timing estimates. T=0.2, and $R(d)$ and $P(d)$ are used in metrics.

	SNR	0 dB	3 dB	6 dB	9 dB
M_1	$\|dt\|<16$	80;85	92;100	89;100	87;100
	$\|dt\|<3$	56;59	78;85	85;95	86;99
	$\|dt\|<2$	46;49	70;76	81;90	85;98
	$\|dt\|<1$	25;26	47;51	64;72	76;88
M_2	$\|dt\|<16$	80;85	92;100	89;100	87;100
	$\|dt\|<3$	66;70	89;97	89;100	87;100
	$\|dt\|<2$	53;57	80;87	86;96	86;99
	$\|dt\|<1$	24;25	42;46	53;60	61;70
M_3	$\|dt\|<16$	80;85	92;100	89;100	87;100
	$\|dt\|<3$	60;64	88;95	89;100	87;100
	$\|dt\|<2$	50;53	81;88	88;98	87;100
	$\|dt\|<1$	26;28	53;57	70;79	80;92

Table 3. Probabilities (%) of correct timing estimates. T=0.2 and b metrics are used.

	SNR	0 dB	3 dB	6 dB	9 dB
M_1	$\|dt\|<16$	86;87	99;100	98;100	97:100
	$\|dt\|<3$	67;68	94;94	98;99	97;100
	$\|dt\|<2$	54;55	85;85	95;97	97;100
	$\|dt\|<1$	27;27	52;53	75;76	89;92
M_2	$\|dt\|<16$	87;87	99;100	98;100	97;100
	$\|dt\|<3$	72;72	96;97	98;100	97;100
	$\|dt\|<2$	58;58	86;87	95;96	96;99
	$\|dt\|<1$	26;26	45;46	59;60	68;70
M_3	$\|dt\|<16$	87;87	99;100	98;100	97;100
	$\|dt\|<3$	69;70	96;97	98;100	97;100
	$\|dt\|<2$	56;57	88;88	96;98	97;100
	$\|dt\|<1$	27;27	51;52	69;71	81;83

In Table 4, we have results when T=0.4 has been used. Because no false alarms exist, we have only one value in each cell. Also, the threshold is too large for SNR=0 dB and these results are not presented. We see that the performance declines more than 10% when SNR is 3 dB and $|dt|<2$. Instead, more correct timing estimates are achieved when the SNR is larger. While metrics M_1 and M_2 attain better performance by lack of false alarms alone, metric M_3 achieves an additional performance gain. This may be explained by the fact that T is used in M_3 calculation (11). This separates metric M_3 from other used metrics. We see, again, that there are no significant differences with the results if we let $|dt|>1$. If we desire $|dt|<1$, metric M_1 or M_3 should be used. These offer about 20% performance improvement at the SNR 9 or 12 dB.

Table 5 shows results for threshold T=0.6. In this time the performance has declined even when SNR is 6 dB. Again, M_3 has attained a few percentage performance gain when the SNR is 9 or 12 dB and $|dt|<1$. We see that the proposed novel metric slightly outperforms M_1 in this case.

Table 4. Probabilities (%) of correct timing estimates. T=0.4 and b metrics are used.

	SNR	3 dB	6 dB	9 dB	12 dB
M_1	$\|dt\|<16$	83.4	100	100	100
	$\|dt\|<3$	79.1	99.5	99.99	100
	$\|dt\|<2$	71.6	96.8	99.7	100
	$\|dt\|<1$	44.4	76.0	92.1	98.5
M_2	$\|dt\|<16$	83.4	100	100	100
	$\|dt\|<3$	81.1	99.9	100	100
	$\|dt\|<2$	72.7	96.3	99.4	99.97
	$\|dt\|<1$	38.4	59.8	70.0	78.3
M_3	$\|dt\|<16$	83.4	100	100	100
	$\|dt\|<3$	79.8	99.9	100	100
	$\|dt\|<2$	72.7	98.1	99.9	100
	$\|dt\|<1$	45.0	76.7	91.0	97.6

Table 5. Probabilities (%) of correct timing estimates. T=0.6 and b metrics are used.

	SNR	3 dB	6 dB	9 dB	12 dB
M_1	$\|dt\|<16$	0.2	85.8	100	100
	$\|dt\|<3$	0.2	85.4	99.99	100
	$\|dt\|<2$	0.2	83.1	99.7	100
	$\|dt\|<1$	0.1	65.5	92	98.5
M_2	$\|dt\|<16$	0.2	85.8	100	100
	$\|dt\|<3$	0.2	85.7	100	100
	$\|dt\|<2$	0.2	82.8	99.4	99.97
	$\|dt\|<1$	0.1	51.6	70.0	78.3
M_3	$\|dt\|<16$	0.2	85.8	100	100
	$\|dt\|<3$	0.2	85.5	100	100
	$\|dt\|<2$	0.2	83.6	99.9	100
	$\|dt\|<1$	0.1	66.2	93.6	99.2

V. CONCLUSIONS

Timing synchronization procedures were presented for the WIND-FLEX prototype consisting of one transmitter and one receiver. The novel low-complex timing metric was presented and compared to some other metrics via simulation results. The simulation model considered the presented control architecture and the AWGN channel. In simulations certain training symbols have been used. Different results may appear for various training symbols.

All metrics using 128 samples in energy $R_b(d)$ calculation have nearly similar performance if an inaccuracy of multiple sample intervals is accepted. For instance, 95 % of all frames achieve timing accuracy of ±2 samples from the optimal timing instant, when SNR is 3 dB and threshold is 0.2. Use of larger thresholds, 0.4 or 0.6, decreases the number of detected frames at SNRs of 3 dB and 6 dB, respectively.

If the optimal timing instant is desired, the novel metric outperforms the MC metric at SNRs equal to or larger than 3 or 6 dB. The performance gain increases as the SNR gets larger values. Our metric has a performance loss compared to the MNC metric if threshold 0.2 is used at SNRs higher than or equal to 6 dB. At lower SNRs the MC or the novel metric should be used. When the threshold is 0.4, the MNC and our metric have nearly equal performance. As the threshold is 0.6, our metric slightly outperforms the MNC metric. Results show that the novel metric achieves more accurate estimates at high enough SNRs as the threshold increases. Other simulated metrics obtain performance gain only by experiencing less false alarms in frame detection.

The novel timing metric is implemented in the WIND-FLEX prototype. In addition to its estimation accuracy, it offers a less complex implementation than the MNC metric. Further work will be done for the WIND-FLEX demonstrator. We shall separate fine-tuning (e.g. tracking) from timing acquisition. By this way more estimation accuracy and robustness should be introduced for a multipath channel. Also, the implementation should consume less power.

ACKNOWLEDGEMENTS

This work has been carried out in the IST-1999-10025 WIND-FLEX project, which is partly funded by the European Commission. The authors wish to thank Sandrine Boumard and Aarne Mämmelä for offering their state-of-the-art knowledge on OFDM synchronization in the early phase of this work, and Ilkka Saarinen for his valuable comments on this paper.

REFERENCES

[1] R. van Nee and R. Prasad, "OFDM Wireless Multimedia Communications", Artech House, 2000, 260 pp.

[2] L. Hanzo, W. Webb, and T. Keller: "Single- and multi-carrier quadrature amplitude modulation", John Wiley&Sons, Chichester, 2000.

[3] T.M. Schmidl and D.C. Cox, "Robust Frequency and Timing Synchronization for OFDM", IEEE Transactions on Communications, Vol. 45, No. 12, Dec. 1997.

[4] S. Boumard and A. Mämmelä, "Timing Acquisition Methods for WLAN OFDM Performance and Comparisons", in Proceedings of SoftCOM 2001 Conference, Oct. 9-12, 2001, Croatia and Italy, Vol. 1, pp. 455 - 462.

[5] S.H. Müller-Weinfurtner, "On the Optimality of Metrics for Coarse Frame synchronization in OFDM: A comparison", in Proceedings of PIMRC'98, Sep. 8-11, Vol. 2, pp. 191-193. (Presentation slides from http://www.uwsmw.de/pub_stefan.html)

[6] S.H. Müller-Weinfurtner, "Sandwich Preamble for Burst Synchronization", in Proceedings of 5th International OFDM-Workshop, Hamburg, Germany, Sep. 2000, pp. 23.1-23.4.

[7] T. Keller and L. Hanzo, "Orthogonal Frequency Division Multiplex Synchronisation Techniques for Wireless Local Area Networks", in Proceedings of PIMRC'96, Taipei, Taiwan, Oct. 1996, pp. 963-967.